Available online at www.sciencedirect.com
ScienceDirect
Journal of Molecular Catalysis A: Chemical 283 (2008) 120–128
JOURNAL OF MOLECULAR CATALYSIS A: CHEMICAL
www.elsevier.com/locate/molcata

Host (nanocage of zeolite–Y)/guest (manganese(II), cobalt(II), nickel(II) and copper(II) complexes of 12-membered macrocyclic Schiff-base ligand derived from thiosemicarbazide and glyoxal) nanocomposite materials: Synthesis, characterization and catalytic oxidation of cyclohexene

Masoud Salavati-Niasari [a,b,*]

[a] *Institute of Nano Science and Nano Technology, University of Kashan, Kashan, P.O. Box 87317-51167, Islamic Republic of Iran*
[b] *Department of Chemistry, Faculty of Science, University of Kashan, Kashan, P.O. Box 87317-51167, Islamic Republic of Iran*

Received 8 September 2007; received in revised form 4 December 2007; accepted 6 December 2007
Available online 23 December 2007

Abstract

A series of Mn(II), Co(II), Ni(II) and Cu(II) complexes with 12-membered macrocyclic tetradentate ligand; $H_6C_6N_6S_2$ = 1,2,5,6,8,11-hexaazacyclododeca-7,12-dithione-2,4,8,10-tetraene; have been synthesized and characterized as homogeneous and encapsulated into the nanopores of zeolite–Y. These catalytic systems show a good activity in the oxidation of cyclohexene to 2-cyclohexene-1-one, 2-cyclohexene-2-ol and 1-(*tert*-butylperoxy)-2-cyclohexene. The chelation of zeolite-exchanged metal(II) by N-containing ligand gives rise to a whole class of Host–Guest Nanocomposite Materials (HGNM) as heterogeneous liquid-phase oxidation, which exhibits similar catalytic performances than the homogeneous ones. The encapsulated complexes abbreviated here as [M($H_4C_6N_6S_2$)]–NaY, catalyze the oxidation of cyclohexene using TBHP as oxidant in good yield. Cyclohexene catalyzed by [M($H_4C_6N_6S_2$)]–NaY under optimized reaction conditions gave three reaction products namely, 2-cyclohexene-1-one, 2-cyclohexene-2-ol and 1-(*tert*-butylperoxy)-2-cyclohexene. In the presence of *tert*-butylhydroperoxide all catalysts gave 2-cyclohexene-1-one in major yield, though overall conversion has been found low (40–90%).

Keywords: Nanocomposite materials; 12-Membered macrocycle; Zeolite encapsulation; Oxidation of cyclohexene

1. Introduction

Host (nanopores of zeolite)/Guest (redox transition metal complexes) Nanocomposite Materials (HGNM) and related materials are one of the subjects of current catalysis research due to their potentiality as biomimetic heterogeneous catalysts for the oxidation of alkanes, alkenes and alcohols [1–10]. The hybrid organic–inorganic material (or HGNM) not only has heterogeneous catalysis characteristics, but also retains high catalytic efficiency originating in homogeneous catalysis due to the site-isolated effect. In addition, the steric constraints imposed on the transition metal complex by zeolite nanochannels, the negative charge of the zeolite framework and distribution of the positive charge of the cations as well as surface properties of the zeolite can also lead to specific interactions, inducing structural and functional modification, as compared to pure complexes [11].

So far several approaches have been taken for the encapsulation of transition metal complexes in nanocages of zeolites [1–3]. The choice of a specific method is dictated by size of ligand relative to the free diameter of the zeolite channels. The Flexible Ligand Method (FLM) is a straightforward and simple strategy. The FLM is based on the principle that the free ligand guests can easily enter into the nanocavities of the zeolite host material because they are flexible enough to pass through the restricting windows giving access to the larger cages (Scheme 1). However, once the ligand has entered in the zeolite cage and chelated with the previously exchanged transition metal ions, the formed complex is unable to escape from the zeolite host matrix due to its much larger size than zeolite nanopore diameter [12].

Encapsulation of transition metals in nanoporous materials has drawn considerable interests since this process gives rise

* Correspondence address: Department of Chemistry, Faculty of Science, University of Kashan, Kashan, P.O. Box 87317-51167, Islamic Republic of Iran. Tel.: +98 361 5555 333; fax: +98 361 5552 930.
E-mail address: salavati@kashanu.ac.ir.

1381-1169/$ – see front matter © 2007 Elsevier B.V. All rights reserved.
doi:10.1016/j.molcata.2007.12.015

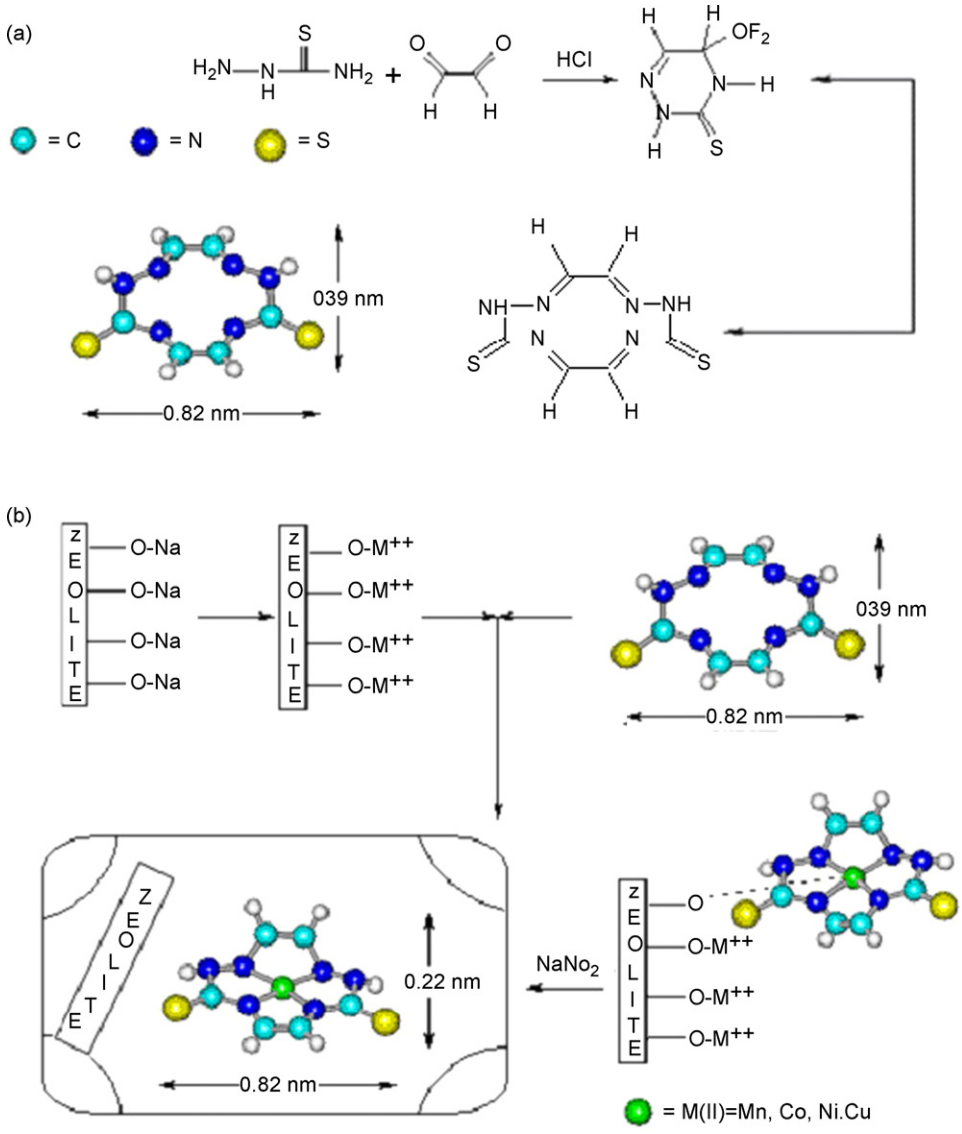

Scheme 1.

to materials with acid and/or redox property [13–17]. However, a serious problem, namely leaching of the active component of metal ions, happened to these redox molecular sieves in the process of liquid-phase oxidation reactions [14]. This problem shortens the catalyst life. Effective prevention of metal leaching from redox molecular sieves during the liquid-phase oxidation of alkanes, alkenes and alcohols with H_2O_2 as an oxidant is a challenge in heterogeneous catalysis. The encapsulation approach is convenient and ideal because the complex, once formed inside the nanocages of the zeolite, is too large to diffuse out and is not lost into the liquid-phase during the reaction. As these composite materials mimic biological enzymes, they are also called "zeozymes" (acronym for zeolite mimics of enzymes). On confinement in the zeolite matrix, the metal complex may lose some of its degrees of freedom and adopt unusual geometries that are stabilized by coordination to the zeolite functional groups. In a general sense, the encapsulated complexes mimic enzyme systems in that the nanoporous inorganic mantle (similar to the protein mantle in enzymes) provides (hopefully) the right steric requirement for the metal complex and imposes certain requirements (based on size and shape) to the access of the active site by the substrate molecules (substrate selectivity). Though many porous materials have been used, the most popular ones have been zeolite–Y possessing large cages (1.2 nm diameters).

I undertook this work for two principal reasons; (i) the heterogenization of the homogeneous catalysis for having the benefit of easy catalyst separation and (ii) explore the possibility of macrocyclic complexes catalyzed oxidation reaction (shape selective) which has not been examined so far with these complexes. In this paper, I report my results on "FLM" synthesis of $[M(H_4C_6N_6S_2)]$; $H_6C_6N_6S_2$ = 1,2,5,6,8,11-hexaazacyclododeca-7,12-dithione-2,4,8,10-tetraene; encapsulated in nanocavity of zeolite–Y (Scheme 1) and their its application in oxidation of cyclohexene.

2. Experimental

2.1. Materials

Metal salts were commercial products of highest chemical grade (Fluka). Solvents were purified according to standard procedures. Thiosemicarbazide and glyoxal were procured from Fluka. All the solvents were purchased from Merck (pro analysi) and were distilled and dried using molecular sieves (Linda 4 Å). Reference samples of cyclohexanol and cyclohexanone were distilled and stored in the refrigerator. NaY with the Si:Al ratio of 2.53 was purchased from Aldrich (Lot No. 67812).

2.2. Physical measurements

FT-IR spectra were recorded on Shimadzu Varian 4300 spectrophotometer in KBr pellets. Electronic spectra of the neat complexes; [$M(H_4C_6N_6S_2)$]; were taken on a Shimadzu UV–Vis scanning spectrometer (Model 2101 PC). Diffuse reflectance spectra (DRS) were registered on a Shimadzu UV/3101 PC spectrophotometer the range 1500–200 nm, using MgO as reference. The elemental analysis (carbon, hydrogen and nitrogen) of the materials was obtained from Carlo ERBA Model EA 1108 analyzer. XRD patterns were recorded by a Rigaku D-max C III, X-ray diffractometer using Ni-filtered Cu Kα radiation. Nitrogen adsorption measurements were performed at 77 K using a Coulter Ofeisorb 100CX instrument. The samples were degassed at 150 °C until a vacuum better than 10^{-3} Pa was obtained. Micropore volumes were determined by the *t*-method, a "monolayer equivalent area" was calculated from the micropore volume [18,19]. The stability of the encapsulated catalyst was checked after the reaction by UV–Vis and possible leaching of the complex was investigated by UV–Vis in the reaction solution after filtration of the zeolite. The amounts of metallocomplexes encapsulated in zeolite matrix were determined by the elemental analysis and by subtracting the amount of metallocomplex left in the solutions after the synthesis of the catalysts as determined by UV–Vis spectroscopy, from the amount taken for the synthesis. Atomic absorption spectra (AAS) were recorded on a PerkinElmer 4100–1319 Spectrophotometer using a flame approach, after acid (HF) dissolution of known amounts of the zeolitic material and SiO_2 was determined by gravimetric analysis. Magnetic moments were calculated from magnetic susceptibility data obtained using a Johnson Matthey MK-1 magnetic susceptibility balance and conductance measurements with a Metrohm Herisau conductometer E 518.

2.3. Synthesis of intermediate ligand, 6-ethoxy-4-thio-2,3,5-triazine [20]

An ethanolic (50 ml) solution of thiosemicarbazide (0.01 mol, 0.92 g) was added to ethanolic (50 ml) solution of glyoxal (0.01 mol, 0.58 g) with constant stirring in the presence of 25 ml of 2 M hydrochloric acid. The mixture was heated with stirring for 8 h. On keeping it overnight at room temperature, a yellowish brown colored crystalline solid was formed. The solid was filtered, washed with ethanol and dried in vacuum over P_4O_{10} (Scheme 1).

2.4. Synthesis of 12-membered macrocyclic ligand; $H_6C_6N_6S_2$ = 1,2,5,6,8,11-hexaazacyclododeca-7,12-dithione-2,4,8,10-tetraene [20]

An ethanolic (50 ml) solution of copper(II) chloride (0.002 mol, 0.35 g) was added to an ethanolic (50 ml) suspension of intermediate ligand, 6-ethoxy-4-thio-2,3,5-triazine (0.002 mol, 0.29 g). The mixture was stirred at room temperature until the cream solid 1,2,5,6,8,11-hexaazacyclododeca-7,12-dithione-2,4,8,10-tetraene formed. The product was filtered, washed with ethanol and dried in vacuum over P_4O_{10} (Scheme 1).

2.5. Preparation of neat 12-membered macrocyclic complexes [$M(H_4C_6N_6S_2)$] (M = Mn(II), Co(II), Ni(II), Cu(II))

A hot ethanolic solution (10 ml) of corresponding metal acetate (0.001 mol) was added to a hot ethanolic (10 ml) suspension of 12-membered macrocyclic ligand (0.001 mol, 0.23 g). The mixture was refluxed for 2 h. On cooling a colored complex precipitated out. The precipitated complex was filtered, washed with ethanol and dried in vacuum over P_4O_{10}.

2.6. Preparation of M(II)–NaY (M = Mn, Co, Ni, Cu)

M(II)–NaY was prepared by ion-exchange method. Typically, 3.2 mmol manganese acetate was dissolved in 400 ml deionized water. Then, 20 g NaY was added to the solution, and further stirred for 24 h at ambient temperature. The solid product was filtered out, washed with deionized water until the filtrate was free from any free metal ion on the surface of the zeolite, and dried at 120 °C for 12 h.

2.7. Preparation of HGNM; [$M(H_4C_6N_6S_2)$]–NaY

The encapsulated complex was prepared using general FLM [21,22]. About 1.0 g M(II)–NaY and 1.2 g of $H_6C_6N_6S_2$ = 1,2,5,6,8,11-hexaazacyclododeca-7,12-dithione-2,4,8,10-tetraene; were mixed in a round-bottomed flask. The reaction mixture was heated at 250 °C (14 h) in an oil bath with stirring. The melted ligand acted as solvent as well as reactant. The resulting material was taken out and extracted with methanol until the complex was free from the unreacted $H_6C_6N_6S_2$. The resulted zeolites, were Soxhlet extracted with *N*,*N*′-dimethylformamide (for 4 h) and with ethanol (for 3 h) to remove excess unreacted diamine and any M(II) complexes adsorbed onto the external surface of the zeolite crystallites. The uncomplexed M(II) ions present in the zeolite were removed by exchanging with aqueous 0.01 M NaCl solution. The resulting solid was washed with hot distilled water until no precipitation of AgCl on treating filtrate with $AgNO_3$.

The HGNM was dried at 150 °C for several hours to constant weight.

2.8. Homogeneous oxidation of cyclohexene

To a solution of cyclohexene (1 ml), neat metal complex (1.02×10^{-5} mol) in dichloromethane (10 ml), was added TBHP (2 ml). The resulting mixture was refluxed for 8 h under N_2 atmosphere then, the solvent evaporated under reduced pressure and the crude analyzed by GC and GC–MS. The concentrations of products were determined using cyclohexanone as internal standard.

2.9. Heterogeneous oxidation of cyclohexene

A mixture of catalyst (1.02×10^{-5} mol), solvent (25 ml) and cyclohexene (10 mmol) were stirred under nitrogen atmosphere in a 50 ml round-bottom flask equipped with a condenser and a dropping funnel at room temperature for 30 min. Then 16 mmol of TBHP (solution 80% in di-*tert*-butylperoxide) was added. The resulting mixture was refluxed for 8 h under N_2 atmosphere. After filtering and washing with solvent, the filtrate was concentrated and then subjected to GC analysis. The concentration of products was determined using cyclohexanone as internal standard.

3. Results and discussion

3.1. Synthesis and characterization

The elemental and chemical analysis confirmed the purity and the stoichiometry of the neat complexes and HGNM (Table 1). The chemical analysis of the samples reveals the presence of organic matter with a C/N ratio roughly similar to that for neat complexes.

The mol ratios Si/Al obtained by chemical analysis for zeolites are presented (Table 1). The Si and Al contents in M(II)–NaY and the HGNM; [M($H_4C_6N_6S_2$)]–NaY; are almost in the same ratio as in the parent zeolite. The Si/Al ration has remained unchanged indicating the absence of dealumination during ion.

The FLM synthesis, Scheme 1, leads to the encapsulation of manganese(II), cobalt(II), nickel(II) and copper(II) complexes of $[H_4C_6N_6S_2]^{2-}$ ligand within the nanopores of zeolite. The parent NaY zeolite has Si/Al molar ratio of 2.53 which corresponds to a unit cell formula $Na_{56}[(AlO_2)_{56}(SiO_2)_{136}]$ (Table 1). The unit cell formulae of metal-exchanged zeolites show a metal dispersion of around 11 moles per unit cell (Mn(II)–NaY, $Na_{33.2}Mn_{11.3}[(AlO_2)_{56}(SiO_2)_{136}]\cdot nH_2O$; Co(II)–NaY, $Na_{34}Co_{11}[(AlO_2)_{56}(SiO_2)_{136}]\cdot nH_2O$; Ni(II)–NaY, $Na_{33.8}Ni_{11.1}[(AlO_2)_{56}(SiO_2)_{136}]\cdot nH_2O$; Cu(II)–NaY, $Na_{34.4}Cu_{10.8}[(AlO_2)_{56}(SiO_2)_{136}]\cdot nH_2O$). The analytical data of each complex indicate M:C:H molar ratios almost close to those calculated for the mononuclear structure. However, the presence of minute traces of free metal ions in the lattice could be assumed as the metal content is slightly higher than the stoichiometric requirement. Only a portion of metal ions in metal-exchanged zeolite has undergone complexation and the rest is expected to be removed on re-exchange with sodium nitrate solution.

The X-ray diffraction (XRD) patterns of zeolite contained complexes are similar to those of M(II)–NaY and the parent NaY zeolite. The zeolite crystallinity is retained on encapsulating complexes. Crystalline phase of free metal ions or encapsulation ligand complexes were not detected in any of the patterns as their fine dispersion in zeolite might have rendered them non-detectable by XRD.

The ^{1}H NMR spectrum of intermediate ligand in $CDCl_3$ shows two signals at 9.10 and 10.13 ppm corresponding to two secondary amine group. It also shows the presence of ethanol at 3.64 q (CH_2) and 1.63 t (CH_3). The ^{1}H NMR spectrum of $H_6C_6N_6S_2$ is almost to that of intermediate ligand except the signals of ethanol are absent. Their data confirms the 1 + 1 cyclization of intermediate ligand. The isolated solid complexes are stable in air and are insoluble in common organic solvents but soluble in DMF and DMSO. Their molar conductance indicates that all the complexes are non-electrolytes in nature. On heating all the complexes are decomposed and do not give sharp melting point.

The principal IR bands and their assignments were studied for determining the ligand mode of coordination. The absence of bands in the 2600–2800 cm^{-1} region of the IR spectra of $H_6C_6N_6S_2$ and its complexes suggest that the absence of any thiol tautomer in the solid state [23]. The IR spectrum of $H_6C_6N_6S_2$ is similar to intermediate ligand which indicates that $H_6C_6N_6S_2$ is adulterated from intermediate ligand. On complexation formation the band corresponding to $\nu_{C=N}$ shifted towards higher indicating that the coordination takes place through azomethine nitrogen. The $\nu_{C=S}$ band observed at 835 cm^{-1} in the spectrum of the free ligand remains unchanged in the complexes indicating that it does not involve in the coordination [24]. Thus the ligand coordinates through metal through four amine nitrogen atom (Scheme 1). IR spectroscopy provides information on the integrity of the encapsulated complexes, as well as the crystallinity of the host zeolite. The IR bands of all encapsulated complexes (HGNM) are weak due to their low concentration in the zeolite. Transition metal complexes encapsulated in the zeolite nanocages did not show any significant shift in functional groups stretching modes. I did not consider any appreciable changes in the frequencies of metal complexes after incorporation into zeolite matrix.

The magnetic moment of four-coordinate nickel(II) complex at room temperature lies in the −0.018 B.M. corresponding to diamagnetic complex. The complex [Ni($H_4C_6N_6S_2$)] prepared by using nickel acetate is diamagnetic suggesting square-planar geometry [25]. The electronic spectrum of [Ni($H_4C_6N_6S_2$)) complex in Nujol shows bands at 909, 604 and 451 nm assigned to following $1_{A1g} \rightarrow 1_{A2g}$ (ν_1), $1_{A1g} \rightarrow 1_{B2g}$ (ν_2) and $1_{A1g} \rightarrow 1_{Eg}$ (ν_3) transitions, respectively, corresponding to square-planar geometry. However, the electronic spectrum in DMSO is entirely different and shows bands at 1033, 703, 455 nm corresponding to octahedral geometry. It suggests that in solution, the solvent molecules are also coordinated at their axial positions. The magnetic moment of the copper(II)

Table 1
Chemical composition of neat; [Mn($H_4C_6N_6S_2$)]; and Host–Guest Nanocomposite Materials; [Mn($H_4C_6N_6S_2$)]–NaY[a]

Sample	C (%)	H (%)	N (%)	M (%)	C/N	Si (%)	Al (%)	Na (%)	Si/Al
Intermediate ligand	37.70 (37.59)	5.69 (5.52)	26.40 (26.52)	–	1.43, 1.42	–	–	–	–
$H_6C_6N_6S_2$	31.85 (31.62)	2.65 (2.54)	37.14 (37.29)	–	0.86, 0.85	–	–	–	–
NaY	–	–	–	–	–	21.76	8.60	7.50	2.53
Mn(II)–NaY	–	–	–	2.58	–	22.08	8.73	3.34	2.53
[Mn($H_4C_6N_6S_2$)]	25.81 (25.69)	1.43 (1.36)	30.09 (30.20)	19.68 (19.59)	0.86 (0.85)	–	–	–	–
[Mn($H_4C_6N_6S_2$)]–NaY	2.14	0.73	2.82	2.73	0.76	21.24	8.39	5.35	2.53
Co(II)–NaY	–	–	–	–	–	21.53	8.53	3.36	2.53
[Co($H_4C_6N_6S_2$)]	25.45 (25.23)	1.42 (1.30)	29.67 (29.80)	20.81 (20.69)	0.86 (0.85)	–	–	–	–
[Co($H_4C_6N_6S_2$)]–NaY	2.12	0.72	2.90	2.72	0.73	21.25	8.40	5.33	2.53
Ni(II)–NaY	–	–	–	–	–	21.79	8.62	3.28	2.53
[Ni($H_4C_6N_6S_2$)]	25.47 (25.29)	1.41 (1.24)	29.69 (29.77)	20.75 (20.51)	0.86 (0.85)	–	–	–	–
[Ni($H_4C_6N_6S_2$)]–NaY	2.10	0.70	3.09	2.74	0.68	21.23	8.39	5.30	2.53
Cu(II)–NaY	–	–	–	–	–	21.48	8.49	3.28	2.53
[Cu($H_4C_6N_6S_2$)]	25.01 (24.86)	1.39 (1.28)	29.03 (29.18)	22.08 (21.89)	0.86 (0.85)	–	–	–	–
[Cu($H_4C_6N_6S_2$)]–NaY	2.08	0.67	2.89	2.78	0.72	21.20	8.38	5.28	2.53

[a] %Calculated (found %).

Table 2
Vibrations parameters and some physical properties for Schiff-base, neat metal(II) complexes and HGNM

Sample	IR (KBr, cm^{-1})					μ_{eff} (MB)	Λ_M[a] (Ω^{-1} cm^2 M^{-1})	d ↔ d (nm)[b]
	ν(N–H)	ν(C=N)	Thioamide I	Thioamide II	ν(M–N)			
[Mn($H_4C_6N_6S_2$)]	3294, 3082	1638	1519, 1440	837	450	5.94	17	–
[Mn($H_4C_6N_6S_2$)]–NaY	–	1635	–	836	–	–	–	–
[Co($H_4C_6N_6S_2$)]	3290, 3030	1635	1521, 1443	836	452	1.74	23	557, 425
[Co($H_4C_6N_6S_2$)]–NaY	–	1633	–	837	–	–	–	555
[Ni($H_4C_6N_6S_2$)]	3285, 3040	1630	1519, 1444	838	454	−0.018	14	1033, 703, 455
[Ni($H_4C_6N_6S_2$)]–NaY	–	1628	–	839	–	–	–	453
[Cu($H_4C_6N_6S_2$)]	3250, 3160	1662	1520, 1475	838	450	1.85	8	891, 572, 446
[Cu($H_4C_6N_6S_2$)]–NaY	–	1620	–	840	–	–	–	570
Intermediate ligand	3242, 3155	1609	1520, 1465	835	–	–	–	–
$H_6C_6N_6S_2$	3240, 3159	1608	1520, 1466	837	–	–	–	–

[b] In DMSO solution.

complex at room temperature lies in 1.85 B.M., corresponding to one unpaired electron (Table 2). This indicates that these complexes are monomeric in nature and the absence of metal–metal interaction. The complex [Cu($H_4C_6N_6S_2$)] synthesized by using copper(II) acetate exhibit bands at 891, 572 and 446 nm corresponding to the square-planar geometry [25–27], but in DMSO solution spectral bands corresponds to octahedral geometry. It suggests that solvent molecules are also coordinated at their axial positions. The tetrahedral geometry of the [Mn($H_4C_6N_6S_2$)] is strongly indicated by similarities in the visible spectra of this chelate with those of known tetrahedral complexes containing oxygen–nitrogen donor atoms [28]. The spectrum of the [Co($H_4C_6N_6S_2$)] exhibits two bands at 555–660 nm which are assigned to d ↔ d transitions. In addition, a lower energy absorption at 425 nm has been observed such low energy bands which have recently been shown to be characteristic of square-planar cobalt(II) chelates [25,29–32]. This geometry is confirmed by the values of the effective magnetic moment (Table 2). The diffuse reflectance spectra of transition metal complexes are almost identical before and after encapsulation (Table 2), indicating that the complexes maintain their geometry even after encapsulation without significant distortion.

In order to investigate the location of the transition metal thiosemicarbazone complexes within the host material, I conducted nitrogen adsorption experiments with the empty zeolitic host and with different immobilized transition metal complexes. The results are summarized in Table 3. In comparison to the host material, a decrease in the BET surface area and the

Table 3
Surface area and pore volume data of thiosemicarbazone metal(II) complexes encapsulated in nanopores of zeolite–Y

Sample	Surface area (m^2/g)[a]	Pore volume (ml/g)[b]
NaY	545	0.31
Mn(II)–NaY	535	0.30
[Mn($H_4C_6N_6S_2$)]–NaY	413	0.21
Co(II)–NaY	532	0.30
[Co($H_4C_6N_6S_2$)]–NaY	418	0.23
Ni(II)–NaY	528	0.30
[Ni($H_4C_6N_6S_2$)]–NaY	420	0.23
Cu(II)–NaY	532	0.30
[Cu($H_4C_6N_6S_2$)]–NaY	423	0.24

[a] Surface area is the "monolayer equivalent area" calculated as explained in Refs. [18] and [19].
[b] Calculated by the *t*-method.

nanoporous volumes can be detected with all catalysts. According to the nitrogen adsorption data, the guest occupies nanopores of the host material. Since the zeolite framework structure is not affected by encapsulation as shown by the XRD patterns, the reduction of surface area and pore volume provides direct evidence for the presence of complexes in the cavities [33].

3.2. Catalytic activity

The oxidation of cyclohexene is negligible in the absence of $[M(H_4C_6N_6S_2)]$ and HGNM catalysts confirming that under the conditions of the experiments, the oxidation is indeed catalytic in nature. In the case of the encapsulated catalysts, transition metal was not detected in the reaction products by AAS indicating that oxidation of cyclohexene by dissolved transition metal complexes leached out from the zeolite matrix is negligible. The zeolites alone without the transition metal complexes were also catalytically inactive. Since the concentration of uncomplexed transition metal ions in the catalysts is also negligible, their contribution to catalytic activity may be neglected. Further evidence to confirm that the oxidation of cyclohexene is catalyzed to a significant extent by the solid zeolite catalyst containing the encapsulated metal complex and not by the free complex dissolved in solution was obtained as follows: in one set of two identical experiments, the solid catalyst $[Mn(H_4C_6N_6S_2)]$–NaY) was removed by centrifugation after a reaction time of 8 h. While the conversion of cyclohexene proceeded further in the presence of the solid catalyst, there was no further conversion of cyclohexene when the catalyst was removed from the reaction system.

The results in the oxidation of cyclohexene using TBHP as oxidant at reflux over the various catalysts have been given in Tables 4–6. The major products of oxidation are 2-cyclohexene-1-one, 2-cyclohexene-2-ol and 1-(*tert*-butylperoxy)-2-cyclohexene. The zeolite-encapsulated complexes (HGNM) did not undergo any color change during the reaction and could be easily separated and reused many times. In contrast, the neat complexes, while they were active in the first cycle, were completely destroyed during the first run and changed color. The neat complexes gave low conversions compared to the encapsulated catalysts. This may be a consequence of above, since, due to the continuous degradation of the catalyst, the effective concentration of the catalyst will be lower than that taken initially.

Table 4
Oxidation of cyclohexene with TBHP catalyzed by neat thiosemicarbazone metal complexes; $[Cu(H_4C_6N_6S_2)]$; in CH_2Cl_2

Catalyst	Conversion (%)	Selectivity (%)		
		Ketone[a]	Alcohol[b]	Peroxide[c]
$[Mn(H_4C_6N_6S_2)]$	58.5	64.7	22.6	12.7
$[Mn(H_4C_6N_6S_2)]$[d]	37.4	47.3	32.8	19.9
$[Mn(H_4C_6N_6S_2)]$[e]	51.3	66.1	22.6	11.3
$[Mn(H_4C_6N_6S_2)]$[f]	22.1	68.5	21.7	9.8
$[Co(H_4C_6N_6S_2)]$	45.2	55.6	32.0	12.4
$[Ni(H_4C_6N_6S_2)]$	25.6	41.3	42.2	16.5
$[Cu(H_4C_6N_6S_2)]$	37.8	46.7	31.2	22.1

[a] 2-Cyclohexene-1-one.
[b] 2-Cyclohexene-1-ol.
[c] 1-(*tert*-Butylperoxy)-2-cyclohexene.
[d] Catalyst = 0.5×10^{-5} mol.
[e] Catalyst = 2.04×10^{-5} mol.
[f] Catalyst = 4.08×10^{-5} mol.

Table 5
Oxidation of cyclohexene with TBHP catalyzed by HGNM in CH_2Cl_2

Catalyst	Conversion (%)	Selectivity (%)		
		Ketone[a]	Alcohol[b]	Peroxide[c]
$[Mn(H_4C_6N_6S_2)]$–NaY	90.3	87.5	11.5	1.0
$[Mn(H_4C_6N_6S_2)]$–NaY[d]	88.6	86.4	12.4	1.2
$[Mn(H_4C_6N_6S_2)]$–NaY[e]	88.1	85.0	13.7	1.3
$[Mn(H_4C_6N_6S_2)]$–NaY[f]	86.5	83.2	15.4	1.4
$[Co(H_4C_6N_6S_2)]$–NaY	59.3	67.8	23.6	8.6
$[Ni(H_4C_6N_6S_2)]$–NaY	32.6	60.2	29.6	10.2
$[Cu(H_4C_6N_6S_2)]$–NaY	40.1	65.5	22.0	12.5

[a] 2-Cyclohexene-1-one.
[b] 2-Cyclohexene-1-ol.
[c] 1-(*tert*-Butylperoxy)-2-cyclohexene.
[d] First reuse.
[e] Second reuse.
[f] Third reuse.

The results of catalytic oxidation of cyclohexene with TBHP are presented in Table 5. No oxidation products have been observed in blank experiment with pure NaY support, showing that the catalytic activity is associated with the ligand component. In all catalytic experiments with HGNM the reaction mixtures remain colorless. The UV–Vis spectra of the decanted liquid show no presence of the band typical of metallocomplex species. Furthermore, upon addition of a fresh dose of TBHP to the decanted liquid no catalytic effect is observed. These facts indicate that the catalytic activity is associated with metallocomplex centers encapsulated within the nanoporoes of zeolite. The activity of cyclohexene oxidation decreases in the series $[Mn(H_4C_6N_6S_2)]$–NaY > $[Co(H_4C_6N_6S_2)]$–NaY > $[Cu(H_4C_6N_6S_2)]$–NaY > $[Ni(H_4C_6N_6S_2)]$–NaY.

The trend observed in Tables 4 and 5 can be explained by the donor ability of ligand available in the complex catalysts. As Wang and co-workers have pointed out, the key point in the conversion of cyclohexene to the products is the reduction of L-$M^{(n+1)+}$ to L-M^{n+}. This reduction to L-M^{n+} is facilitated with the ligands available around the metal cation [34].

Table 6
Oxidation of cyclohexene with TBHP catalyzed by $[Mn(H_4C_6N_6S_2)]$–NaY in different solvents

Solvent	Conversion (%)	Selectivity (%)		
		Ketone[a]	Alcohol[b]	Peroxide[c]
CH_2Cl_2	90.3	87.5	11.5	1.0
CH_3Cl	84.1	83.0	14.7	2.3
CH_3OH	70.3	67.4	19.9	12.7
CH_3CN	61.4	50.5	35.6	13.9

[a] 2-Cyclohexene-1-one.
[b] 2-Cyclohexene-1-ol.
[c] 1-(*tert*-Butylperoxy)-2-cyclohexene.

The effect of various solvents for the oxidation of cyclohexene with [Mn($H_4C_6N_6S_2$)]–NaY catalysts was also studied (Table 6). In all the oxidation reactions, 2-cyclohexene-1-one was formed as major product. When the reaction was carried out in a coordinating solvent like CH_3CN the conversion decreased by a factor of ∼1.47 because of donor number of acetonitrile (14.1). Therefore, acetonitrile has a higher ability to occupy the vacant spaces around the metal center and prevent the approaching of oxidant molecules. In dichloromethane and chloroform the yields of 2-cyclohexene-1-o1 and 2-cyclohexene-1-one were higher and lower yield of the peoxy species was obtained as compared to the other solvents. The efficiency of the catalysts for cyclohexene oxidation in different solvents decreases in the order: dichloromethane > chloroform > methanol > acetonitrile.

The effect of transition metal complexes encapsulated in zeolite; [M($H_4C_6N_6S_2$)]–NaY; was studied on the oxidation of cyclohexene with TBHP in dichloromethane and the results are shown in Table 5. As shown in Table 5, only allylic oxidation has occurred with the formation of 2-cyclohexene-1-one, 2-cyclohexene-1-ol and 1-(*tert*-butylperoxy)-2-cyclohexene. Oxidation with the same oxidant in the presence of Mn(II)–NaY was 51.4% [35]. The increase of conversion from 51.4% [35] to 90.3% compared to Mn(II)–NaY with [Mn($H_4C_6N_6S_2$)]–NaY indicates that the existence of ligand has increased the activity of the catalyst by a factor of 1.76. From the indicated results in Table 5 it is evident that 2-cyclohexene-1-one is selectively formed in the presence of all catalysts.

The influence of the support on the stability of a metallocomplex catalyst has been investigated on the example of [Mn($H_4C_6N_6S_2$)], by reusing the [Mn($H_4C_6N_6S_2$)]–NaY sample in another catalytic cycle. The experiment has shown that the recycled catalyst maintains high activity, corresponding to 90.3% of the initial value, with unchanged selectivity pattern. In a similar experiment carried out in a reference homogeneous system a large drop of activity to the level of 58.5% is observed. The loss is associated with the decomposition of almost half of the metallocomplex during the first catalytic run, as evidenced by the diminution of the characteristic UV–Vis band. Thus, the effect of supporting consists not only in the change of the selectivity pattern, but also in the stabilisation of the catalytically active metallocomplex species.

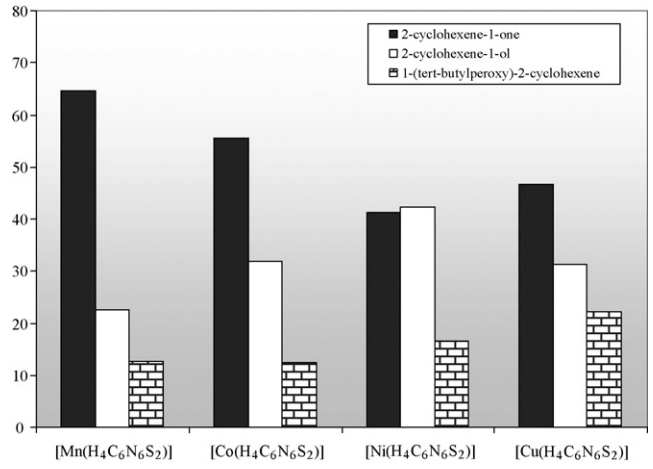

Fig. 1. Oxidation products distribution in dichloromethane with [M($H_4C_6N_6S_2$)]/TBHP.

The formation of the allylic oxidation products 2-cyclohexene-1-one and 2-clohexene-1-ol shows the preferential attack of the activated C–H bond over the C=C bond

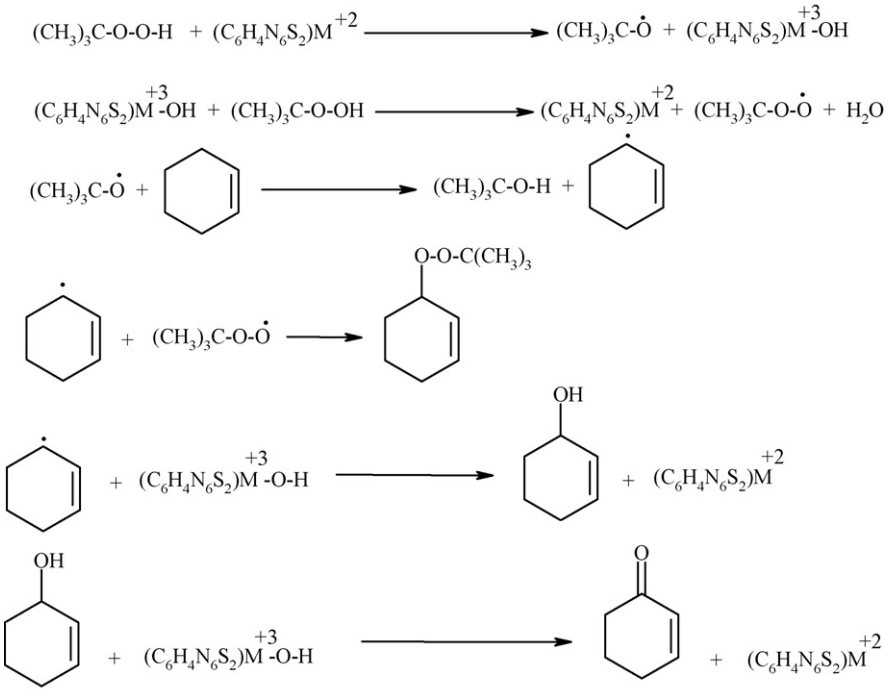

M: Mn, Co, Ni, Cu

Scheme 2.

(Figs. 1 and 2). The formation of 1-(*tret*-butylperoxy)-2-cyclohexene shows the presence of radical reactions [36]. TBHP as oxidant promotes the allylic oxidation pathway and epoxidation decreased, especially under the acidic properties of zeolite encapsulated with divalent and trivalent transition metal ions and complexes, has been observed by others and us [37–41].

The main path of the reaction is oxidation of the allylic position. The reason is clear and can be attributed to the increased acidity of zeolite due to the hydrolysis of hydrated ion, an effect which has been observed by others and us. Leibovich et al. have reported that the exchange of some monovalent ions of silver in zeolite with divalent calcium ions decreases the oxidation yield of cyclohexene to the corresponding epoxide and facilitate the allylic site oxidation [42]. The author has pointed out that increasing acidity of zeolite has been responsible for this change. As mentioned elsewhere, 2-cyclohexene-1-one product should have arisen from the oxidation of 2-cyclohexene-1-ol (Scheme 2). Mn(II)–NaY catalyst shows low tendency to further oxidation of alcohol forming 2-cyclohexene-1-ol under the reaction conditions While $[Mn(H_4C_6N_6S_2)]$–NaY oxidize the alcohol mostly to the ketone.

4. Conclusion

The oxidation of cyclohexene using the thiosemicarbazone complexes of transition metal encapsulated in zeolite–NaY has been investigated. When the oxidation is carried out using *tert*-butylhydroperoxide as the initiator, significant conversion levels were achieved. The products were 2-cyclohexene-1-one, 2-cyclohexene-2-ol and 1-(*tert*-butylperoxy)-2-cyclohexene. The zeolite-encapsulated complexes did not undergo any color change during the reaction and could be easily separated and reused many times. In contrast, the neat complexes, while they were active in the first cycle, were completely destroyed during the run and changed color. The neat complexes; $[Mn(H_4C_6N_6S_2)]$; however, gave low conversions compared to the encapsulated catalysts. The efficiency of the catalysts for oxidation of cyclohexene in different solvents decreases in the order: dichloromethane > chloroform > methanol > acetonitrile.

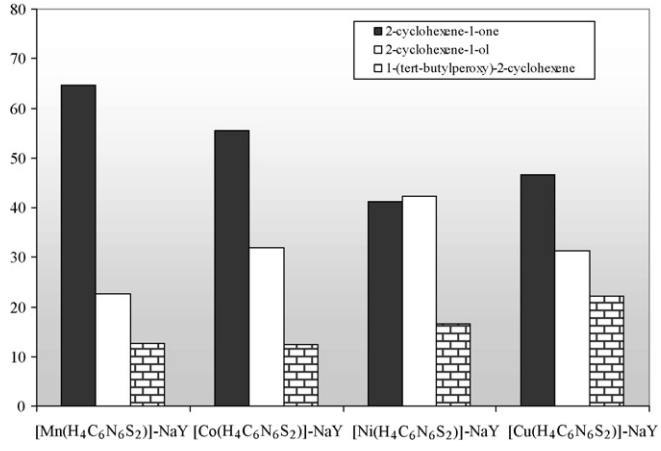

Fig. 2. Oxidation products distribution in dichloromethane with $[M(H_4C_6N_6S_2)]$–NaY/TBHP.

The extension of the method to different olefins is currently under investigation in our laboratory.

Acknowledgment

Author is grateful to Council of University of Kashan for providing financial support to undertake this work.

References

[1] K.J. Balkus Jr., M. Eissa, R. Levado, J. Am. Chem. Soc. 117 (1995) 10753.
[2] M.R. Maurya, A.K. Chandrakar, S. Chand, J. Mol. Catal. A: Chem. 263 (2007) 227.
[3] S.P. Varkey, C. Ratnasamy, P. Ratnasamy, J. Mol. Catal. A: Chem. 135 (1998) 295.
[4] Y. Umemura, Y. Minai, T. Tominaga, J. Phys. Chem. B 103 (1999) 647.
[5] C.R. Jacob, S.P. Varkey, P. Ratnasamy, Appl. Catal. A: Gen. 182 (1999) 91.
[6] B.V. Romanovsky, Proceedings of the 8th International Congress on Catalysis, Verlag Chiemie, Weinheim, 1984, p. 657.
[7] N. Herron, G.D. Stucky, C.A. Tolman, J. C. S. Chem. Commun. (1986) 521.
[8] M. Salavati-Niasari, J. Mol. Catal. A: Chem. 229 (2005) 159.
[9] M. Salavati-Niasari, Inorg. Chem. Commun. 9 (2006) 268.
[10] M. Salavati-Niasari, J. Mol. Catal. A: Chem. 245 (2006) 192.
[11] R. Grommen, P. Manikandan, Y. Gao, T. Shane, J.J. Shane, R.A. Schoonheydt, B.M. Weckhuysen, D. Goldfarb, J. Am. Chem. Soc. 122 (2000) 11488.
[12] G. Schulz-Ekloff, S. Ernst, in: G. Ertl, et al. (Eds.), Handbook of Heterogeneous Catalysis, Wiley–VCH, Weinheim, 1997, p. 374.
[13] W. Fan, B.M. Weckhuysen, R.A. Schoonheydt, Chem. Commun. (2000) 2249.
[14] M.J. Haanepen, A.M. Elemans-Mehring, J.H.C. van Hooff, Appl. Catal. A: Gen. 152 (1997) 183.
[15] K.J. Chao, A.C. Wei, H.C. Wu, J.F. Lee, Catal. Today 49 (1999) 277.
[16] M. Salavati-Niasari, Inorg. Chem. Commun. 7 (2004) 963.
[17] M. Salavati-Niasari, M. Bazarganipour, Catal. Commun. 8 (2006) 336.
[18] S.W. Wang, H. Everett, R.A.W. Haul, L. Moscou, R.A. Pierotti, J. Rouquerol, T. Siemieniewska, Pure Appl. Chem. 57 (1985) 603.
[19] J.A. Moulijn (Ed.), Carbon and Coal Gasification, Martinus Nijhoff, Dordrecht, MA, 1986, p. 137.
[20] S. Chandra, X. Sangeetika, Spectrochim. Acta Part A 60 (2004) 147.
[21] C.R. Jacob, S.P. Varkey, P. Ratnasamy, Micropor. Mesopor. Mater. 22 (1998) 465, and references therein.
[22] C. Bowers, P.K. Dutta, J. Catal. 122 (1990) 271.
[23] W.J. Geary, Coord. Chem. Rev. 7 (1971) 81.
[24] S.B. Padhye, G.B. Kauffman, Coord. Chem. Rev. 63 (1985) 127.
[25] A.B.P. Lever, Inorganic Electronic Spectroscopy, 2nd ed., Elsevier, Amsterdam, 1984.
[26] M. Salavati-Niasari, J. Mol. Catal. A: Chem. 217 (2004) 87.
[27] M. Salavati-Niasari, Chem. Lett. 34 (2005) 244.
[28] N. Raman, Y.P. Raja, A. Kulandaisamy, Proc. Indian Acad. Sci. (Chem. Sci.) 113 (2001) 183.
[29] C.A. Root, B.A. Rising, M.C. Vanderveer, C.F. Hellmuth, Inorg. Chem. 11 (1972) 1489.
[30] F.L. Urbach, R.D. Bereman, J.A. Topido, M. Hariharan, B.J. Kalbacher, J. Am. Chem. Soc. 92 (1970) 792.
[31] M. Salavati-Niasari, M.R. Ganjali, P. Norouzi, Trans. Met. Chem. 32 (2007) 1.
[32] M. Salavati-Niasari, Chem. Lett. 34 (2005) 1444.
[33] K.J. Balkus, A.G. Gabrielov, J. Incl. Phenom. Mol. Recogn. Chem. 21 (1995) 159.
[34] M. Wang, C.J. Hao, Y.P. Wang, S.B. Li, J. Mol. Catal. A: Chem. 147 (1999) 173.
[35] M. Salavati-Niasari, F. Farzaneh, M. Ghandi, L. Turkian, J. Mol. Catal. A: Chem. 157 (2000) 183.
[36] D. Koola, J.K. Kochi, J. Org. Chem. (1987) 4545.

[37] A.H. Gemeay, M.A. Salem, I.A. Salem, Colloid Surf. 117 (1996) 245.
[38] M. Salavati-Niasari, H. Banitaba, J. Mol. Catal. A: Chem. 201 (2003) 43.
[39] M. Salavati-Niasari, A. Amiri, Appl. Catal. A: Gen. 290 (2005) 46.
[40] M. Salavati-Niasari, P. Salemi, F. Davar, J. Mol. Catal. A: Chem. 238 (2005) 215.
[41] M. Salavati-Niasari, A. Amiri, Trans. Met. Chem. 30 (2005) 720.
[42] H. Leibovich, C. Abaroni, N. Lotun, J. Catal. 87 (1984) 319.